Holocene carbon-cycle dynamics based on CO$_2$ trapped in ice at Taylor Dome, Antarctica

A. Indermühle*, T. F. Stocker*, F. Joos*, H. Fischer†, H. J. Smith†, M. Wahlen†, B. Deck†, D. Mastroianni†, J. Tschumi*, T. Blunier*, R. Meyer* & B. Stauffer*

* *Climate and Environmental Physics, Physics Institute, University of Bern, Sidlerstrasse 5, CH-3012 Bern, Switzerland*
† *Scripps Institution of Oceanography, University of California San Diego, La Jolla, California 92093-0220, USA*

....

A high-resolution ice-core record of atmospheric CO$_2$ concentration over the Holocene epoch shows that the global carbon cycle has not been in steady state during the past 11,000 years. Analysis of the CO$_2$ concentration and carbon stable-isotope records, using a one-dimensional carbon-cycle model, suggests that changes in terrestrial biomass and sea surface temperature were largely responsible for the observed millennial-scale changes of atmospheric CO$_2$ concentrations.

Precise and continuous direct measurements of the concentration of atmospheric CO$_2$ started in 1958, and show a clear increase from 315 parts per million by volume (p.p.m.v.) to 364 p.p.m.v. by 1997[1]. This accumulation of the most important greenhouse gas after water vapour is caused by fossil-fuel burning and changes in land use. For a better understanding of the carbon cycle it is important to know the concentration history of atmospheric CO$_2$ on various timescales. Before 1958, such histories can only be investigated reliably by analysing air enclosed in polar ice. Earlier work showed that the atmospheric CO$_2$ concentration was about 280 p.p.m.v. before the beginning of industrialization[2] and that only small variations of about 5 p.p.m.v. occurred during the pre-industrial part of the past millennium[3,4]. However, the atmospheric CO$_2$ concentration increased from about 200 to 270 p.p.m.v. during the transition from the Last Glacial Maximum (~20 kyr before present, BP) to the beginning of the Holocene (~11 kyr BP)[5]. During the last glacial period, fluctuations of ~20 p.p.m.v. occurred on a millennial timescale from 46 to 18 kyr BP (ref. 6). In contrast, little is known about the CO$_2$ concentrations during most of the Holocene, the current interglacial period[7].

The stable-isotope composition of atmospheric CO$_2$ (δ^{13}C; see Methods for definition) permits the attribution of carbon to different carbon reservoirs. The detection of the fossil-fuel signature (the Suess effect) was first reported by Keeling *et al.*[8]. Direct atmospheric measurements, firn air samples and samples extracted from ice cores revealed a decrease of δ^{13}C from −6.5‰ to −7.8‰ since the beginning of industrialization; they also showed a small century-scale variability during the pre-industrial part of the past millennium[9,10]. Other measurements on ice cores have shown that δ^{13}C increased by ~0.3‰ from the Last Glacial Maximum to the Holocene[11]. The δ^{13}C record, when used in inverse modelling, gives a further constraint on the global carbon budget and allows the calculation of the net fluxes of carbon from the atmosphere to the ocean and to the land biosphere[9,12,13].

Here we present a high-resolution record of CO$_2$ concentrations as measured in air bubbles trapped in an ice core from Taylor Dome, Antarctica, covering the entire Holocene. The record shows a decrease of the CO$_2$ concentration from 268 p.p.m.v. at 10.5 kyr BP (the end of the transition from the last glacial to the Holocene) to 260 p.p.m.v. at 8.2 kyr BP. During the following 7 kyr, the CO$_2$ concentration increased almost linearly to ~285 p.p.m.v. The reproducibility (that is, the standard deviation of the mean) of most of our measurements is better than 1 p.p.m.v. Furthermore, we present a Holocene δ^{13}C record from the same ice core. The record

shows an increase of 0.3‰ from 11 to 8 kyr BP, and a decrease of 0.2‰ over the following 7 kyr. On the basis of inverse modelling we propose that most of the variability in atmospheric CO$_2$ concentration is caused by changes in the amount of land biomass and in sea surface temperature.

Potential *in situ* and analytical artefacts

The reconstruction of atmospheric CO$_2$ concentration from ice cores is not a straightforward procedure owing to the following difficulties. High-resolution measurements of CO$_2$, and the comparison of CO$_2$ records from different ice cores, have shown that the atmospheric CO$_2$ signal can be masked by CO$_2$ production in the ice matrix; such *in situ* production is most likely due to chemical reactions between impurities, collectively referred to as natural artefacts. The physics and chemistry of these processes, documented in ice cores from Greenland[14–16], are little known, but two possible candidates are being investigated. (1) Acid–carbonate reactions[14,16,17] and (2) oxidation of organic matter by H$_2$O$_2$ (ref. 18). The probability of a reaction depends on the concentration of the impurities and their location in the ice (for example, at grain boundaries or associated with dust particles), which are not known in detail for either Greenland or Antarctic cores. But it has been shown that the concentrations of the impurities are one order of magnitude smaller in ice cores from Antarctica than in those from Greenland, so that the probability of natural artefacts is smaller in Antarctic records[14,18,19]. Detailed measurements on a Greenland core (GRIP) have shown an *in situ* CO$_2$-production potential (by an acid–carbonate reaction) of up to 3,000 p.p.m.v., but a CO$_2$ surplus of only 30 p.p.m.v. has been observed[18]. Thus, an existing CO$_2$-production potential does not necessarily mean that a natural artefact occurs. At present, the most promising test to detect such natural artefacts is to perform detailed measurements across a few annual layers. If the measured CO$_2$ concentration represents the atmospheric composition, the variation between adjacent samples should be similar to the analytical uncertainty. If CO$_2$ is produced by chemical reactions, a larger scatter of the data points is likely.

Fractionation of CO$_2$ between bubbles and clathrates may occur in the clathrate-formation zone of the ice, whose depth depends on the local temperature[20]. If the extraction efficiency is below 100%, which is the case with our device, a depletion of CO$_2$ in the extracted air could occur. However, calculations reveal that ice of the Holocene period from Taylor Dome is clearly above the clathrate zone, and so this problem is not relevant.

Samples and chronology

The ice core from Taylor Dome (77° 48′ S, 158° 43′ E; elevation, 2,374 m above sea level; accumulation rate, 7 cm ice equivalent per year, ref. 21)—hereafter referred to as TD—is 554 m long and was drilled in 1993/94 by a US consortium. Due to the low annual mean temperature of −42 °C (ref. 22), the occurrence of melt layers is unlikely. Analyses of the isotopic composition of the ice (δD, a proxy for temperature) reveal that the glacial–interglacial transition is between 375 and 353 m depth[23]. For the Holocene CO_2 record, a total of 417 samples from 69 different depth intervals were measured in Bern. An additional 50 samples from 15 different depth levels were measured in San Diego for interlaboratory comparison. Furthermore, 13 samples were measured in San Diego for the $\delta^{13}C$ record.

The porous firn layer on the surface of an ice sheet is continuously exchanging air with the overlaying atmosphere. Therefore, the air at the bubble close-off depth is younger than the surrounding ice. The present-day close-off depth at TD can be calculated using the model of Martinerie et al.[24] and the density profile of TD[25]; it is located at 72 m. In order to obtain an age of the air enclosed in bubbles,
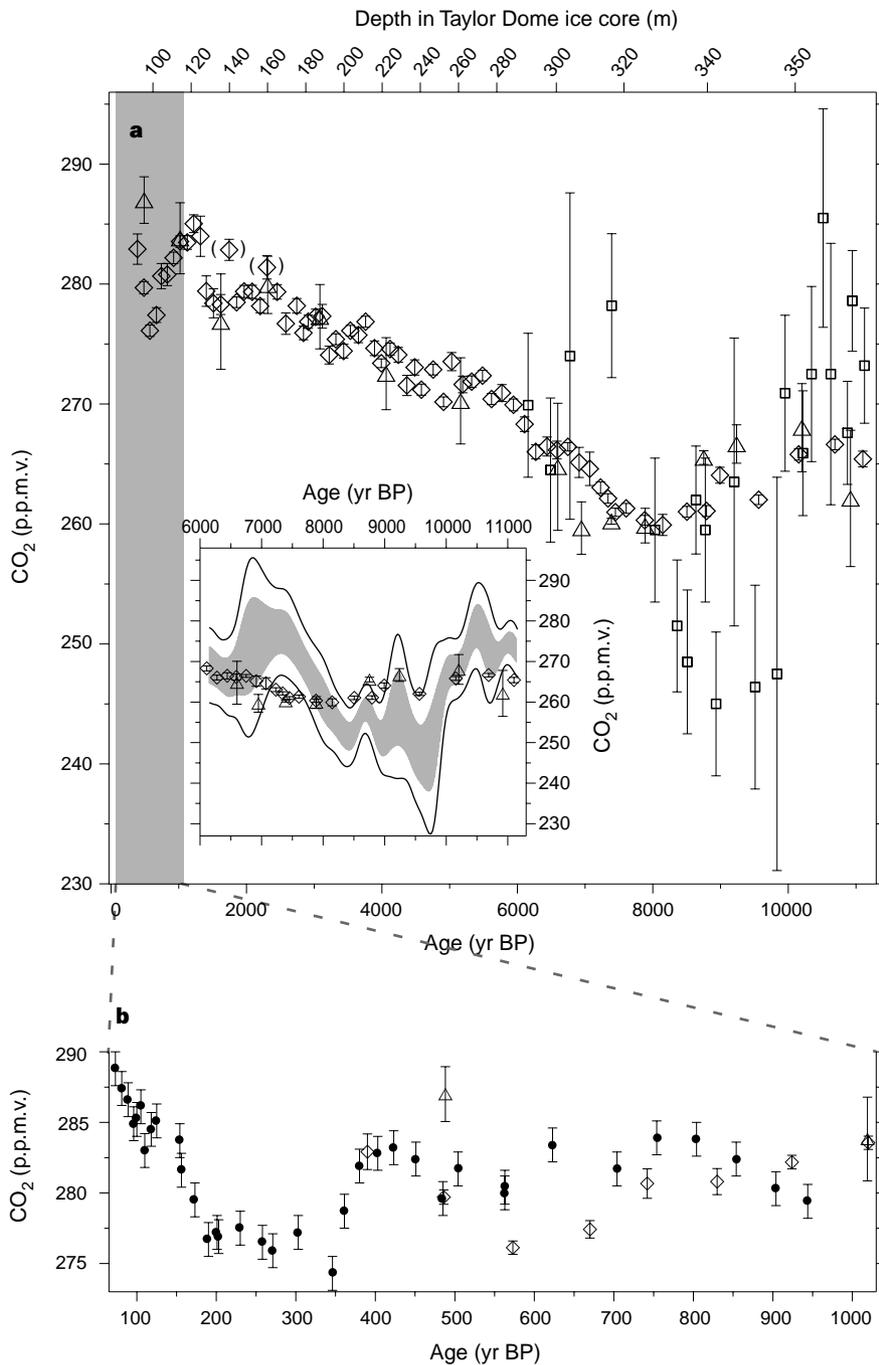
Figure 1 Mean CO_2 concentrations from ice cores. **a**, Open diamonds, mean of five to six samples from Taylor Dome ice core measured in Bern. Open triangles, mean of three to six samples measured in San Diego. Open squares, data from Byrd Station ice core[5]. Error bars, 1σ of the mean. The brackets indicate samples where natural artefacts cannot be excluded. Inset, as **a** but for the interval where the Byrd Station and Taylor Dome data overlap. Using a Monte Carlo method, 1,000 time series of the CO_2 record from Byrd Station were generated and filtered in order to take into account the different enclosure processes at Byrd Station and Taylor Dome, respectively. Shaded area, 1σ band; solid lines, 2σ band. **b**, Expanded-scale view of the data for the past millennium (shaded area in **a**). Open diamonds and triangles, mean CO_2 concentrations from Taylor Dome; dots, CO_2 concentrations from Law Dome[4].

the CH_4 record from TD was synchronized with its well-dated GISP2 counterpart[26], and the age of each CO_2 sample linearly interpolated from the CH_4-based age scale. The uncertainty of the chronology (mainly due to the uncertainty of the synchronization) is <200 yr between 12–8 kyr BP; in this age range, distinct changes in the CH_4 concentration occur (the Younger Dryas event, and the 8,200 yr event) and the resolution of the CH_4 record from TD is high. From 8 to 1 kyr BP, the uncertainty increases to ±500 yr owing to the low resolution and the relatively smaller variation of the CH_4 records (E. J. Brook, personal communication). For the past millennium, we estimate the uncertainty of the chronology at ~100 yr.

Millennial variations of atmospheric CO_2 and $\delta^{13}C$

The measured CO_2 concentrations from TD are plotted in Fig. 1a versus age and depth, together with the CO_2 record from Byrd Station, West Antarctica[5]. The agreement between the values measured in Bern and San Diego is generally good. The most remarkable features of the TD record are the decrease from 268 p.p.m.v. at 10.5 kyr BP to 260 p.p.m.v. at 8.2 kyr BP, and the monotonic increase over the following 7 kyr to 285 p.p.m.v. Our data is in accordance with previously published data of the past millennium from the ice core of Law Dome[4] (Fig. 1b) and with data from the Vostok ice core[7] (not shown), taking into account the uncertainties of the chronology and the concentrations (1.2 p.p.m.v. for Law Dome). On the other hand, the values from Byrd Station and TD differ considerably in the overlapping section (11–6 kyr BP) and require further consideration.

The CO_2 concentration in the Byrd Station record in the period 11–6 kyr BP increases to 285 ± 9 p.p.m.v. at 10.5 kyr BP and shows large concentration changes of up to 40 p.p.m.v. and a minimum concentration of 245 ± 6 p.p.m.v. In contrast, the record from TD is remarkably smooth. In each depth interval we measured six TD samples along a 0.09–0.15 m section of the core corresponding to one or two samples per annual layer. The standard deviations of the six samples are generally smaller than the analytical uncertainty (1.5 p.p.m.v.). In contrast, standard deviations for Byrd Station samples in the section younger than 11 kyr BP are significantly higher than the analytical uncertainty at the time that the older record was measured (3 p.p.m.v.)[6]. The clathrate-formation zone at Byrd is between 700 and 1000 m (a gas age of 6.5–10.5 kyr BP) as indicated by the bad core quality[5], and coincides with the region where data from Byrd and TD differ. The high scatter of the Byrd record could be explained by a combination of natural artefacts, fractionation in the clathrate-formation zone, or post-coring effects due to the brittleness of the core. We conclude that the Byrd record in the time interval 6–11 kyr BP is much less reliable than the TD record.

We have therefore good evidence that the TD record represents the atmospheric CO_2 concentration with great reliability because (1) the scatter of the adjacent measurements is statistically in agreement with the analytical uncertainty, (2) no clathrates occur in the part of TD discussed here, and (3), the TD record is in general agreement with the sparser Vostok record[7]. (We note that the San Diego measurements show an increased scatter due to the higher analytical uncertainty, see Methods).

In the interval 11–6 kyr BP, the mean values of CO_2 concentration from the Byrd core show similar oscillations to the TD core, but with much larger amplitude. The question arises as to whether both records represent the evolution of atmospheric CO_2, and differ only because of the different enclosure characteristics at the two drilling sites. The enclosure process acts as a low-pass filter, and can be expressed by a normalized Gauss filter with a time constant of $\tau_{BS} = 27$ yr for Byrd Station[27] and $\tau_{TD} = 140$ yr for Taylor Dome, respectively. For a better comparison of the two records, the following procedure was carried out. Assuming that the data from Byrd Station represent the atmospheric CO_2 concentration within the error bars, we generated 1,000 time series of the existing data

using a Monte Carlo method. The expected synthetic TD record was obtained by filtering the time series in order to take into account the different enclosure processes. The resulting 1σ and 2σ bands yield the record within which the TD values would fall if the Byrd CO_2 data between 11 and 6 kyr BP were a true atmospheric record. This can be compared with the measured CO_2 from TD (Fig. 1a, inset). More TD data points than expected from normal distribution are outside the 1σ and 2σ bands. Thus the difference between the two records is probably not due to the different enclosure processes.

In summary, the salient feature of the TD CO_2 record—a decrease of 8 p.p.m.v. from 11 to 8 kyr BP, and a subsequent increase by 25 p.p.m.v. over the following 7 kyr (Fig. 2a)—is the atmospheric imprint of an evolving global carbon cycle.

The measured $\delta^{13}C$ values from TD show an increase from −6.6‰ at 11 kyr BP to −6.3‰ at 8 kyr BP, and then a gradual decrease to −6.5‰ at 1 kyr BP. There is no overlap between $\delta^{13}C$ from TD and Law Dome, but it seems that the TD values are in good agreement with those from Law Dome at 1 kyr BP (− 6.440‰ ± 0.013‰)[10]. The data from TD at 11 kyr BP are in good agreement with the early Holocene average from Byrd (− 6.65‰ ± 0.07‰)[11]. Corrections made to the raw isotopic data include a correction for oxygen isotopes, a gravitational separation correction (using interpolated $\delta^{15}N$ data[23,28]), and a correction for the daily (machine) offset of the air standard. An additional N_2O correction is based on measurements with mixtures of CO_2 and N_2O, from which we have calculated the magnitude of the correction as a function of N_2O/CO_2. We use the published values of N_2O concentration in air[29] as the raw data from which we calculate the corrections for N_2O in our samples. Measurements on different samples from the same depth, as well as measurements of standards, revealed an uncertainty of the $\delta^{13}C$ data of ±0.085‰, including fractionation effects during the extraction and the uncertainty of the $\delta^{15}N$ data.
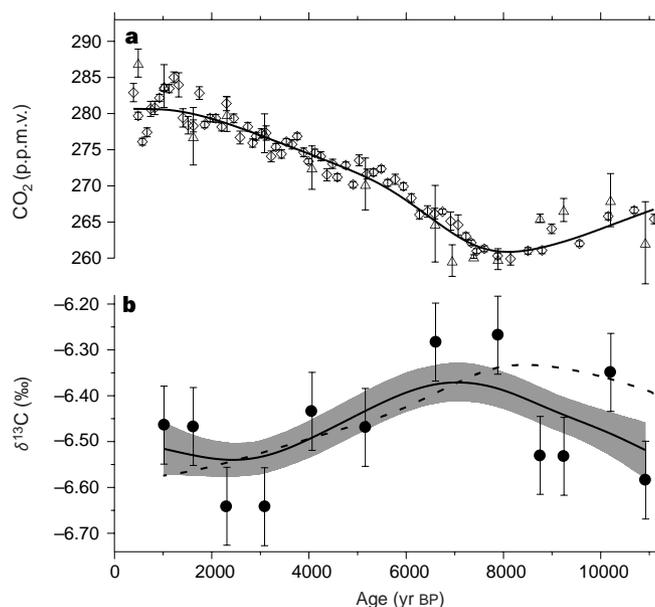
Figure 2 CO_2 concentrations and stable-isotope ratios, Taylor Dome. **a**, CO_2 concentrations. Open diamonds and triangles, mean CO_2 concentration. Error bars, 1σ of the mean. Solid line, spline fit[48] of the CO_2 results used as input for the single and double deconvolution. This spline fit method acts as a low-pass filter; parameters were selected to obtain a cut-off period of ~8,000 yr which is consistent with the low resolution of the $\delta^{13}C$ record. **b**, Measured and calculated $\delta^{13}C$. Filled circles, $\delta^{13}C$ values. Error bars, estimate of the reproducibility of the $\delta^{13}C$ values. Solid line and shaded area, input values of $\delta^{13}C$ for the Monte Carlo simulation. Dashed line, $\delta^{13}C$ calculated with the single deconvolution[31] (land-biosphere-only hypothesis, h1; see text).

Mechanisms of change

The main sources and sinks of atmospheric CO_2 on a millennial timescale are the land biosphere and the ocean. Atmospheric CO_2 concentrations and $\delta^{13}CO_2$ are approximately in dynamical equilibrium with the surface ocean, as dictated by the distribution of dissolved inorganic carbon and ^{13}C, alkalinity, temperature and salinity in the surface ocean[30]. Changes in atmospheric CO_2 concentrations and $\delta^{13}C$ can be caused by changes in terrestrial biomass, in physical processes such as meltwater input, surface ocean warming, changes in air–sea gas exchange and ocean circulation, and in the marine biogeochemical cycles of organic matter and calcite ($CaCO_3$). Consequently, a suite of palaeoclimatic observations would be necessary to quantify the contribution of these individual processes to the observed atmospheric changes. However, budget calculations of C and ^{13}C allow us to validate at least the consistency of explanations for the observed atmospheric CO_2 and $\delta^{13}C$ changes.

Inverse methods (referred to as single[31] and double deconvolution[13]), based on a version of the Bern carbon-cycle model[32], were applied to interpret quantitatively the observed CO_2 and $\delta^{13}C$ variations. As a minor modification, it is assumed that 70% of the carbon released by the land biota during the Holocene is absorbed by sediments on an exponential timescale of 5 kyr (ref. 33). The ocean part of the model includes two surface boxes, representing low- and high-latitude surface water masses. We note that the millennial timescale of the observed atmospheric variations is comparable to the timescale of ocean overturning and is several orders of magnitude longer than atmosphere–surface ocean exchange. Thus, the atmosphere–ocean system is always very close to equilibrium, and results are insensitive to the assumed surface-to-deep transport rates and air–sea exchange coefficients.

Our inverse modelling results presented below suggest that the observed atmospheric variations during the Holocene were driven by a combination of growth (11–7 kyr BP) and decay of terrestrial biomass, and by an increase in sea surface temperature (SST) of ~0.5 °C between 9 and 6 kyr BP. In addition, the slow re-equilibration between the ocean and sediment systems in the wake of the glacial–interglacial transition[34] may also have contributed.

We explored quantitatively four hypotheses, where the atmospheric variations are driven entirely by variation in the land biomass (h1), or by a combination of terrestrial changes plus variations in either SST (h2), the $CaCO_3$ cycle (h3) or the marine organic carbon cycle (h4). Furthermore, a simple estimate shows that meltwater input from ice-sheet remains had a marginal effect on atmospheric CO_2 and $\delta^{13}C$ during the Holocene. The input of melt water reduces sea surface salinity, alkalinity and dissolved inorganic carbon by dilution of the ocean water. Between 10.5 and 8.2 kyr BP, sea level rose ~26 m (ref. 35). Assuming a well-mixed ocean and chemically pure melt water (that is, a maximum dilution effect), the corresponding meltwater input would cause no change in atmospheric $\delta^{13}C$ and a decrease of the atmospheric CO_2 concentration of 2.8 p.p.m.v. (ref. 36), which is clearly less than observed.

Land biota. In the land-biota-only hypothesis (h1), the ocean reacts solely in a passive way to the Holocene atmospheric CO_2 variations. It is assumed that the carbon cycle was in equilibrium at 11 kyr BP, and that the physical and biological properties of the ocean remained unmodified during the Holocene. The carbon uptake of the ocean for slowly varying concentrations of atmospheric CO_2 is then dictated by its chemical capacity to absorb carbon released into the atmosphere–ocean system. The inverse method (single deconvolution[31]) is used for quantification. The net carbon release by the land biosphere then equals the observed rate of change in atmospheric CO_2 (time derivative of solid line in Fig. 2a) plus the modelled uptake by the ocean. The change in atmospheric $\delta^{13}C$ (dashed line in Fig. 2b) is calculated applying time-invariant isotopic fractionation of 18.7‰ (ref. 13). The comparison of measured and modelled $\delta^{13}C$ permits a first test of our hypothesis

(Fig. 2b). From 11 to 6 kyr BP, the calculated increase of 0.06‰ is much smaller than the measured increase of 0.3‰. On the other hand, there is a rather good agreement from about 6 to 1 kyr BP. This agreement implies that the ocean carbon cycle probably operated on a millennial timescale in a remarkably constant mode after 6 kyr BP. Short-term fluctuations induced CO_2 concentration perturbations of less than ±5 p.p.m.v. The calculated cumulative biospheric carbon release during 7–1 kyr BP is 260 Gt C (not shown). We conclude that the observed increase of CO_2, and the $\delta^{13}C$ decrease, from 6 to 1 kyr BP can be explained consistently by terrestrial biosphere forcing only, but that additional mechanisms must be considered to explain the CO_2 and $\delta^{13}C$ changes between 11 and 6 kyr BP.

Sea surface temperature. A change of SST by 1 °C causes a change in the surface ocean's CO_2 partial pressure by 4.2% (ref. 36) which translates into an atmospheric change of similar magnitude[37]. A SST-only model for the observed CO_2 evolution would require a gradual decrease of global mean SST from 10.5 to 8.2 kyr by 0.7 °C and then an increase of 2.3 °C during the following 7 kyr. However, this is not compatible with the $\delta^{13}C$ data. An increase in SST of 2.3 °C would correspond to an increase in the air–sea equilibrium fractionation factor, and thus in atmospheric $\delta^{13}C$, of about 0.25‰ (ref. 38). Instead, TD data show a decrease from 8 to 1 kyr BP. Thus, SST can not have been the only mechanism for the observed changes, although it could have contributed significantly.

Alkenone palaeothermometry[39] and temperature reconstructions from bore-hole measurements in Greenland ice[40] indicate a significant warming during the first part of the Holocene. To test the land biota–SST hypothesis (h2), we performed a double deconvolution[13] where both CO_2 and $\delta^{13}C$ (solid lines in Fig. 2a, b) are used to calculate the two unknown net carbon fluxes into the ocean and into the terrestrial biosphere. Therefore, the assumption of a steady-state natural carbon cycle (as used in the single deconvolution) can be relaxed. SST is then calculated in the model by requiring consistency between simulated net air-to-sea carbon flux and simulated (very small) air–sea CO_2 partial-pressure difference. This means that changes in the sea-surface partial pressure of CO_2, as driven by changes in dissolved inorganic carbon and SST, are forced to be approximately equal to the atmospheric changes. An exponential relationship between partial pressure and SST, based on the thermodynamics of carbonate
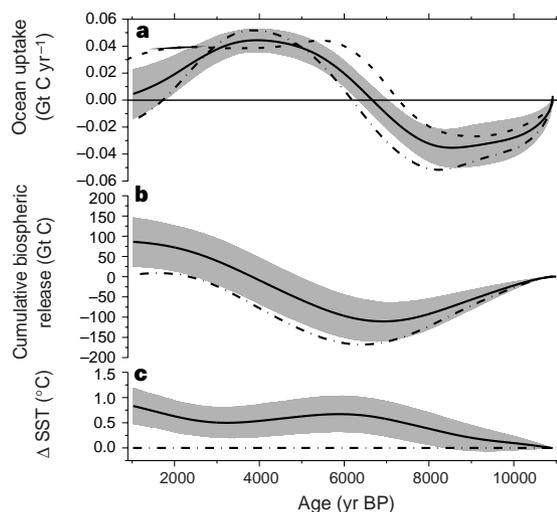
Figure 3 Comparison of our hypotheses. Dashed lines, land-biosphere-only hypothesis (h1). Solid lines, land biota–SST hypothesis (h2). The shaded areas indicate the 1σ confidence interval of a Monte Carlo analysis, taking into account the uncertainty of the ice-core data. Dash-dotted lines, land biota-calcite hypothesis (h3). **a**, Ocean uptake. **b**, Cumulative biospheric release. **c**, Required change in SST.

chemistry[36], is applied. Air–sea fractionation factors are described as functions of SST[38]. A Monte Carlo simulation[13] including 2,000 model runs was performed to assess the uncertainties in the net fluxes introduced mainly by the uncertainty of the $\delta^{13}C$ data (Figs 2 and 3: best estimate, solid lines; shaded area, 1σ bands). SST (Fig. 3c) remained nearly constant during 11–9 kyr BP and after 6 kyr BP, whereas it increased by about 0.5 °C between 9 and 6 kyr BP, roughly in agreement with alkenone palaeothermometry reconstructions[39]. Significant deviations between the single- (land-biota-only hypothesis, h1) and the double-deconvolution results for the combined land biota–SST hypothesis h2 are only found between 8 and 5.5 kyr BP (Fig. 3a, dashed line and shaded area). About one-third of the atmospheric $\delta^{13}C$ increase is explained by the warming of the ocean surface, while the rest is driven by terrestrial carbon uptake. A cumulative biospheric uptake (solid line/shaded area in Fig. 3b) of 110 ± 47 Gt C between 11 and 7 kyr, and a release of 195 ± 40 Gt C between 7 and 1 kyr, is obtained.

Marine biological cycle. It has been suggested that the ocean–sediment system continued to adjust towards a new equilibrium after the glacial–interglacial transition[34]. The observed $\delta^{13}C$ changes cannot be due to a change in the marine calcite cycle only, however, because the isotopic ratio of biogenic calcite is very close to that of ocean surface water. Next, we investigate the land biota–calcite hypothesis (h3) by adjusting the partial pressure of surface-water CO_2 towards the atmospheric pressure as for h2, but without varying SST in the double deconvolution. Again, the atmospheric observations suggest that changes in the land biota alone were responsible for the variations before 9 kyr BP and after 6 kyr BP, as shown by the rather close agreement between the ocean uptake for the land-biota only case (h1; dashed line in Fig. 3a) and the land biota–calcite hypothesis (h3; dot-dashed line in Fig. 3a). For the period 9–6 kyr BP, a significant contribution from variations in the calcite cycle is required. The result is not consistent with the expectation of a system adjusting slowly towards a new equilibrium, in which the contribution by calcite changes to the observed trends would be largest at the beginning of the record. However, uncertainties due to the scarcity of $\delta^{13}C$ data are significant. Our results suggest that adjustments in the calcite cycle after the glacial–interglacial transition may have contributed to the overall atmospheric variations, but did not play the dominant role.

An increase of the export of organic matter from the ocean's surface layer to the deep sea would lead to a decrease of the concentration of atmospheric CO_2 and an increase in atmospheric $\delta^{13}C$. If the decrease of CO_2 of 8 p.p.m.v. from 10.5 to 8.2 kyr BP and the increase of 25 p.p.m.v. from 8.2 to 1 kyr BP were caused by changes in the marine organic carbon cycle only, then $\delta^{13}C$ would first increase by 0.08‰ and then decrease by 0.25‰ (ref. 11). This is not in quantitative agreement with the $\delta^{13}C$ measurements, as the required increase of $\delta^{13}C$ is too small by a factor of 3. We investigate a land biota–marine organic cycle hypothesis (h4) by adjusting the partial pressure of surface water CO_2 towards the atmospheric pressure (as for h2) by varying the export production of marine biota instead of SST in the double deconvolution. Net fluxes for this hypothesis are up to 0.12 Gt C yr^{-1} and are thus much higher than for hypotheses h1–h3. The close correlation between the export production and the terrestrial net flux, as suggested by hypothesis h4, implies a close phase relationship between the two. However, there is no indication that such a strong coupling exists.

Sensitivity. How sensitive are our results to model parameters? We have varied model parameters for our preferred land biota–SST hypothesis (h2). As discussed previously, the results are not sensitive to surface-to-deep ocean mixing and air–sea exchange coefficient. One remaining model parameter is the air–biota fractionation factor. We assumed that the released biogenic material originates from C3 plants, implying an air–biota fractionation factor of 18.7‰ (ref. 13). Changes in calculated sinks were small when this fractionation factor was set to 10‰, assuming that two-thirds of the

released biogenic material (of the order of 100 Gt C) originated from C4 plants[41]. We also varied the air–biota fractionation factor by ± 0.1‰ kyr^{-1} to account for possible transient changes in fractionation that affected all vegetation and soil pools (of the order of 2,000 Gt C). In both cases, we calculated significant deviations of the net carbon fluxes between the standard case (h2) and the sensitivity runs: ~25% from 11 to 7 kyr BP, and ~40% from 7 to 1 kyr BP. The resulting additional uncertainty of the cumulative biospheric release is ± 30 Gt C at 7 kyr BP, and ± 75 Gt C at 1 kyr BP. The additional uncertainty in the required change in SST is ± 0.2 °C at 7 kyr BP, and ± 0.5 °C at 1 kyr BP.

Discussion

The global carbon cycle has not been in steady state during the past 11 kyr. On the basis of our model estimates, we suggest that the observed variations of CO_2 and $\delta^{13}C$ over this period are caused by a combination of growth and decay of terrestrial biomass, and an increase in global mean SST, possibly with a contribution from the marine calcite cycle.

The biospheric uptake of carbon between 11 and 7 kyr BP is consistent with expectations based on vegetation regrowth and soil build-up on areas initially covered by ice sheets, as well as a climatic development towards the mid-Holocene optimum. The simulated uptake of 110 Gt C corresponds to roughly 20% of the estimated glacial–interglacial change in terrestrial storage of 500 Gt C (ref. 42). The cumulative biospheric release of 195 Gt C from 7 to 1 kyr BP could be due to a change from the warmer and wetter mid-Holocene climate to colder and drier conditions. Such changes in northern subtropical regions have been inferred from pollen, lake-level and CH_4 data[43,44]. The changes of the vegetation types in northern Africa and the Arabian peninsula in the past 6.8 kyr have recently been reconstructed, indicating a development from steppe and savannah to desert[45]. Using a biosphere model[46], we calculate carbon storage of 9.5×10^{-6} Gt C km^{-2} in warm grass/shrub, 11×10^{-6} Gt C km^{-2} in tropical dry forest/savannah, and 7.3×10^{-6} Gt C km^{-2} in desert. A difference of about 30 Gt C stored in this area between 6.8 kyr BP and today can be estimated, which is much less than that calculated with our double deconvolution procedure. If our hypothesis is correct, regions in addition to northern Africa and the Arabian peninsula should have contributed substantially to the changes in the terrestrial biosphere.

The rate of change of atmospheric CO_2 concentration over the Holocene is two orders of magnitude smaller than the anthropogenic CO_2 increase since industrialization. Understanding modifications of the distribution of biomes due to past and future climate change is becoming increasingly important, and could be investigated using models of the terrestrial biosphere. The Taylor Dome CO_2 and $\delta^{13}C$ records would serve as important checks for results derived from such models. □

Approximately 200 g of carefully trimmed ice is crushed under vacuum in a rotary, inwardly spiked cylinder in a −26 °C freezer for 30 min. The CO_2 content of the air thus liberated from the ice is extracted on a glass vacuum rack by passing it through a −90 °C acetone/liquid nitrogen (LN) trap to remove water and two −196 °C LN traps to trap the CO_2. The CO_2 is transferred from the first −196 °C trap to the second by warming the first to −90 °C, then into a Pyrex sample tube cooled to −196 °C which is flame sealed. This sample is analysed on a mass spectrometer (VG PRISM II IRMS) for isotopic composition of C and O. $\delta^{13}C = [(^{13}C/^{12}C)_{sample}/(^{13}C/^{12}C)_{standard}] - 1$, referred to the marine carbonate standard PDB.

1. Keeling, C. D. & Whorf, T. P. in *Trends '93: A compendium of Data on Global Change* (eds Boden, T. A., Kaiser, D. P., Sepanski, R. J. & Stoss, F. W.) 16–26 (Carbon Dioxide Information Analysis Center, Oak Ridge, 1994); update available at ⟨http://cdiac.esd.ornl.gov/ndps/ndp001.html⟩.
2. Neftel, A., Moor, E., Oeschger, H. & Stauffer, B. Evidence from polar ice cores for the increase in atmospheric CO_2 in the past two centuries. *Nature* **315**, 45–47 (1985).
3. Barnola, J.-M. *et al.* CO_2 evolution during the last millennium as recorded by Antarctic and Greenland ice. *Tellus B* **47**, 264–272 (1995).
4. Etheridge, D. M. *et al.* Natural and anthropogenic changes in atmospheric CO_2 over the last 1000 years from air in Antarctic ice and firn. *J. Geophys. Res.* **101**, 4115–4128 (1996).
5. Neftel, A., Oeschger, H., Staffelbach, T. & Stauffer, B. CO_2 record in the Byrd ice core 50,000–5,000 years BP. *Nature* **331**, 609–611 (1988).
6. Stauffer, B. *et al.* Atmospheric CO_2 concentration and millennial-scale climate change during the last glacial period. *Nature* **392**, 59–62 (1998).
7. Barnola, J.-M., Pimienta, P., Raynaud, D. & Korotkevich, Y. S. CO_2-climate relationship as deduced from the Vostok ice core: a re-examination based on new measurements and on a re-evaluation of the air dating. *Tellus B* **43**, 83–90 (1991).
8. Keeling, C. D., Mook, W. G. & Tans, P. P. Recent trends in the $^{13}C/^{12}C$ ratio of atmospheric carbon dioxide. *Nature* **277**, 121–123 (1979).
9. Francey, R. J. *et al.* Changes in oceanic and terrestrial carbon uptake since 1982. *Nature* **373**, 326–330 (1995).
10. Francey, R. J. *et al.* A 1000 year high precision record of $\delta^{13}C$ in atmospheric CO_2. *Tellus* (in the press).
11. Leuenberger, M., Siegenthaler, U. & Langway, C. C. Carbon isotope composition of atmospheric CO_2 during the last ice age from an Antarctic ice core. *Nature* **357**, 488–490 (1992).
12. Keeling, C. D., Whorf, T. P., Wahlen, M. & Plicht, J. v. d. Interannual extremes in the rate of rise of atmospheric carbon dioxide since 1980. *Nature* **375**, 666–670 (1995).
13. Joos, F. & Bruno, M. Long-term variability of the terrestrial and oceanic carbon sinks and the budgets of the carbon isotopes ^{13}C and ^{14}C. *Glob. Biogeochem. Cycles* **12**, 277–295 (1998).
14. Anklin, M., Barnola, J.-M., Schwander, J., Stauffer, B. & Raynaud, D. Processes affecting the CO_2 concentrations measured in Greenland ice. *Tellus B* **47**, 461–470 (1995).
15. Smith, H. J., Wahlen, M., Mastroianni, D. & Taylor, K. C. The CO_2 concentration of air trapped in GISP2 ice from the Last Glacial Maximum-Holocene transition. *Geophys. Res. Lett.* **24**, 1–4 (1997).
16. Smith, H. J., Wahlen, M., Mastroianni, D., Taylor, K. C. & Mayewski, P. The CO_2 concentration of air trapped in Greenland Ice Sheet Project 2 ice formed during periods of rapid climate change. *J. Geophys. Res.* **102**, 26577–26582 (1997).
17. Delmas, R. J. A natural artefact in Greenland ice-core CO_2 measurements. *Tellus B* **45**, 391–396 (1993).
18. Tschumi, J. & Stauffer, B. Reconstructing the past atmospheric CO_2-concentration based on ice core analyses: open questions due to in situ production of CO_2 in the ice. *J. Glaciol.* (submitted).
19. Raynaud, D. *et al.* The ice record of greenhouse gases. *Science* **259**, 926–934 (1993).
20. Miller, S. L. Clathrate hydrates of air in Antarctic ice. *Science* **165**, 489–490 (1969).
21. Steig, E. J., Morse, D. L., Waddington, E. D. & Polissar, P. J. Using the sunspot cycle to date ice cores. *Geophys. Res. Lett.* **25**, 163–166 (1998).
22. Waddington, E. D. & Morse, D. L. Spatial variations of local climate at Taylor Dome, Antarctica: Implications for paleoclimate from ice cores. *Ann. Glaciol.* **20**, 219–225 (1994).
23. Steig, E. J. *et al.* Sychronous climate changes in Antarctica and the North Atlantic. *Science* **282**, 92–95 (1998).
24. Martinerie, P. *et al.* Air content paleo record in the Vostok ice core (Antarctica): A mixed record of climatic and glaciological parameters. *J. Geophys. Res.* **99**, 10565–10576 (1994).
25. Fitzpatrick, J. J. Preliminary report on the physical and stratigraphic properties of the Taylor Dome ice core. *Antarct. J. US* **29**, 84–86 (1994).
26. Brook, E. J., Severinghaus, J., Harder, S. & Bender, M. Atmospheric methane and millennial scale climate change. In *Mechanisms of Millennial Scale Climate Change* (Monogr, Am. Geophys. Union, Washington DC, in the press).
27. Schwander, J. & Stauffer, B. Age difference between polar ice and the air trapped in its bubbles. *Nature* **311**, 45–47 (1984).
28. Sucher, C. M. *Atmospheric Gases in the Taylor Dome Ice Core: Implications for East Antarctic Climate Change* Thesis, Univ. Rhode Island (1997).
29. Leuenberger, M. & Siegenthaler, U. Ice-age atmospheric concentration of nitrous oxide from an Antarctic ice core. *Nature* **360**, 449–451 (1992).
30. Broecker, W. S. & Peng, T.-H. *Tracers in the Sea* (Lamont-Doherty Geological Observatory, Palisades, 1982).
31. Bruno, M. & Joos, F. Terrestrial carbon storage during the past 200 years: A Monte Carlo analysis of CO_2 data from ice core and atmospheric measurements. *Glob. Biogeochem. Cycles* **11**, 111–124 (1997).
32. Joos, F. An efficient and accurate representation of complex oceanic and biospheric models of anthropogenic carbon uptake. *Tellus B* **48**, 397–417 (1996).
33. Archer, D., Kheshgi, H. & Maier-Reimer, E. Multiple timescales for neutralization of fossil fuel CO_2. *Geophys. Res. Lett.* **24**, 405–408 (1997).
34. Archer, D. & Maier-Reimer, E. Effect of deep-sea sedimentary calcite preservation on atmospheric CO_2 concentration. *Nature* **367**, 260–263 (1994).
35. Bard, E. *et al.* Deglacial sea-level record from Tahiti corals and the timing of global meltwater discharge. *Nature* **382**, 241–244 (1996).
36. Takahashi, T., Olafson, J., Goddard, J. D., Chipman, D. W. & Sutherland, S. C. Seasonal variation of CO_2 and nutrients in the high-latitude surface oceans: A comparative study. *Glob. Biogeochem. Cycles* **7**, 843–878 (1993).
37. Bacastow, R. B. The effect of temperature change of the warm surface waters of the oceans on atmospheric CO_2. *Glob. Biogeochem. Cycles* **10**, 319–333 (1996).
38. Mook, W. G. ^{13}C in atmospheric CO_2. *Neth. J. Sea Res.* **20**, 211–223 (1986).
39. Bard, E., Rostek, F. & Sonzogni, C. Interhemispheric synchrony of the last deglaciation inferred from alkenone palaeothermometry. *Nature* **385**, 707–710 (1997).
40. Dahl-Jensen, D. *et al.* Past temperatures directly from the Greenland ice sheet. *Science* **282**, 268–271 (1998).
41. Farquhar, G. D., Ehleringer, J. R. & Hubick, K. T. Carbon isotope discrimination and photosynthesis. *Annu. Rev. Plant Physiol. Plant Mol. Biol.* **40**, 503–537 (1989).
42. Crowley, T. J. Ice age terrestrial carbon changes revisited. *Glob. Biogeochem. Cycles* **9**, 377–389 (1995).
43. Street-Perrott, F. A. & Perrott, R. A. in *Global Climates Since the Last Glacial Maximum* (ed. Wright, H. E.) 318–356 (Univ. Minnesota Press, Minneapolis, 1993).
44. Blunier, T., Chappellaz, J., Schwander, J., Stauffer, B. & Raynaud, D. Variations in atmospheric methane concentration during the Holocene epoch. *Nature* **374**, 46–49 (1995).
45. Hoelzmann, P. *et al.* Mid-Holocene land-surface conditions in northern Africa and the Arabian peninsula: A data set for the analysis of biogeophysical feedbacks in the climate system. *Glob. Biogeochem. Cycles* **12**, 35–51 (1998).
46. Esser, G. & Lautenschlager, M. Estimating the change of carbon in the terrestrial biosphere from 18000 BP to present using a carbon cycle model. *Environ. Pollut.* **83**, 45–53 (1994).
47. Wahlen, M., Allen, D., Deck, B. & Herchenroder, A. Initial measurements of CO_2 concentrations (1530 to 1940 AD) in air occluded in the GISP2 ice core from Central Greenland. *Geophys. Res. Lett.* **18**, 1457–1460 (1991).
48. Enting, I. G. On the use of smoothing spline to filter CO_2 data. *J. Geophys. Res.* **92**, 10977–10984 (1987).